Self-Assembled Metal/Molecule/Semiconductor Nanostructures for Electronic Device and Contact Applications

D.B. JANES,[1] TAKHEE LEE,[2] JIA LIU,[3] M. BATISTUTA,[1] NIEN-PO CHEN,[2] B.L. WALSH,[1] R.P. ANDRES,[3] E.-H. CHEN,[1,4,5] M.R. MELLOCH,[1,4] J.M. WOODALL,[1,4,5] and R. REIFENBERGER[2]

1.—Purdue University, School of Electrical and Computer Engineering, W. Lafayette, IN 47907. 2.—Purdue University, Department of Physics, W. Lafayette, IN 47907. 3.—Purdue University, School of Chemical Engineering, W. Lafayette, IN 47907. 4.—Purdue University, NSF MRSEC for Technology Enabling Heterostructure Materials, W. Lafayette, IN 47907. 5.—New address: Yale University, Department of Electrical Engineering, New Haven, CT 06520

We report a fabrication approach in which we combine self-assembled metal/molecule nanostructures with chemically stable semiconductor surface layers. The resulting structures have well controlled dimensions and geometries (~ 4 nm Au nanoclusters) provided by the chemical self-assembly and have stable, low-resistance interfaces realized by the chemically stable semiconductor cap layer (low-temperature grown GaAs passivated by the organic tether molecules). Scanning tunneling microscope imaging and current-voltage spectroscopy of nanocontacts to n-GaAs fabricated using this approach indicate high quality, ohmic nanocontacts having a specific contact resistance of $\sim 1 \times 10^{-7}\ \Omega \cdot cm^2$ and a maximum current density of $\sim 1 \times 10^7\ A/cm^2$, both comparable to those observed in large area contacts. Uniform 2-D arrays of these nanocontact structures have been fabricated and characterized as potential cells for nanoelectronic device applications.

Key words: Self-assembly, nanocluster, ohmic contact, GaAs, STM

INTRODUCTION

Self-assembly techniques provide a means to realize structures such as quantum dots and other electronic/optoelectronic device configurations. Because these techniques do not rely on lithography to realize the specific nanostructures and assemblies, they can represent efficient, high throughput fabrication approaches. There are two classes of self-assembly which have attracted interest for electronic device and materials applications. The first class involves the formation of semiconductor quantum dots either through controlled growth techniques such as the Stranski-Krastanow (S-K) growth technique[1,2] or by deposition of semiconductor materials into regular arrays of pores in an insulating matrix.[3] This approach provides an interesting material, namely arrays of quantum dots, but typically does not lend itself to the assembly of specific device structures or interconnected devices. For self-assembled semiconductor structures, the electronic device functionality has been limited by the difficulty in achieving suitable interfaces for passivating and contacting the resulting islands or dots. A second class of self-assembly approaches involves the formation of semiconductor or metal nanoclusters and 2-D or 3-D assemblies of these clusters.[4–6] It has been shown that the resistive linking between adjacent metal clusters in a 2-D network can be controlled by the choice of intercluster linking molecule[4] and that specific dimer/trimer structures can be realized.[7] In addition, room-temperature Coulomb blockade has been realized in self-assembled metal/molecular nanostructures.[8] However, to date structures based on metal or semiconductor clusters have not provided the types of functionalities provided by semiconductor devices.

In this paper, we describe a self-assembly approach in which metal/molecule nanostructures are utilized to define semiconductor device and contact structures. The overall goal of this approach is to combine the uniform nanostructures that can be realized with self-assembly with the robust functionality provided by semiconductor device structures (gain, directionality, etc.) to realize functional nanoscale devices and interconnections. The resulting structures have well controlled dimensions and geometries (provided by

(Received October 14, 1999; accepted December 27, 1999)

the chemical self-assembly) and have stable, low-resistance interfaces realized by the chemically stable semiconductor cap layers and additional passivation provided by organic tether molecules. As examples of the high quality interfaces and controlled nanometer scale structures which can be realized, we will describe the formation and characterization of nanoscale ohmic contacts to e-type GaAs and close-packed array of metal nanoclusters coupled to GaAs device layers.

METAL/MOLECULE/SEMICONDUCTOR NANOSTRUCTURES

We have developed a number of self-assembled structures using metal nanoclusters and organic molecules.[4,8–10] Nanometer-diameter Au clusters are synthesized using an aerosol reactor known as a multiple expansion cluster source (MECS). Clusters with controlled diameters in the range of 2–20 nm can be synthesized in the MECS; the clusters used in this study are ~4 nm. In the MECS, bare Au clusters are nucleated, grown, and annealed in an inert gas (helium or argon) at reduced pressures. Each cluster is an fcc crystal, faceted in the shape of a truncated octahedron. The bare Au clusters are encapsulated and protected from agglomeration by spraying a surfactant (e.g., dodecanethiol) solution into the aerosol flow downstream of the MECS. Detailed descriptions of the MECS can be found elsewhere.[11] The dodecanethiol encapsulated Au nanoclusters are soluble and form stable colloidal solutions in many nonpolar organic solvents, such as hexane, heptane, chloroform, mesitylene, etc. These encapsulated Au nanoclusters behave like simple chemical compounds; they can be precipitated, re-dissolved, and chromatographically separated without any apparent damage.[12]

Compared to various liquid phase synthesis methods,[12,13] this aerosol synthesis has the following advantages: (1) the clusters are synthesized and annealed at very high temperatures so that each cluster is a well-faceted fcc single crystal; (2) the clusters are charge neutral, which eliminates potential offset charge problems; (3) both bare and encapsulated nanoclusters can be obtained, enabling studies on the effects of encapsulation on the crystal structure and other properties of the nanoclusters; (4) the encapsulant can be displaced by a linking molecule in order to control the structural and electronic properties of the cluster networks.[4]

We have been able to fabricate large-area (spanning a distance of ~1 cm) hexagonal close-packed monolayer arrays and micrometer-sized well-ordered bilayer and multilayer arrays of dodecanethiol encapsulated Au nanoclusters using a two-step procedure. First, a Langmuir-Blodgett (LB) technique[14,15] is used to form an array of encapsulated nanoclusters on a water surface. Next, the array is transferred onto a solid substrate by briefly touching the substrate to the array floating on the water surface.[10]

Self-assembled monolayers (SAMs)[16] of organic molecules have been utilized on semiconductors for both lithographic and passivation purposes.[17] SAMs

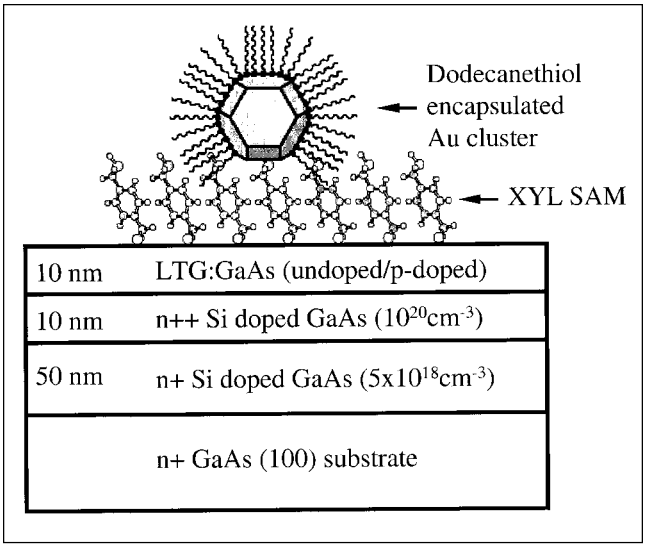

Fig. 1. A schematic diagram of the nanocontact structure showing the GaAs epitaxial layers, the xylyl dithiol monolayer, and the deposited Au cluster encapsulated with dodecanethiol.

of alkanethiols have been used as self-developing electron beam resists on GaAs.[17] In these studies, the protection of the surface was incomplete, primarily due to the fact that stoichiometric GaAs rapidly oxidizes upon exposure to air. In the current work, we employ a SAM of xylyl dithiol ($HS\text{-}CH_2\text{-}C_6H_4\text{-}CH_2\text{-}SH$, denoted as XYL) as a molecular tether and a chemically stable semiconductor surface layer consisting of low-temperature grown GaAs (LTG:GaAs). The XYL monolayer provides a thiol (-SH) end group at both ends; one end bonds to the GaAs surface and the other can tether a Au nanocluster to the surface. The LTG:GaAs, i.e. GaAs grown at a temperature of 250–300°C by molecular beam epitaxy,[18] shows many interesting electronic properties that have been attributed to the ~1–2% excess arsenic incorporated during growth.[18] For as-grown material, the excess arsenic results in a high concentration ($\sim 1 \times 10^{20}$ cm^{-3}) of point defects, primarily as arsenic antisite defects. These defects are observed as a band of states located in the GaAs band gap. These "mid-gap" states prevent the GaAs surface from rapidly oxidizing due to the relatively low concentration of minority carrier holes in the surface layer.[19,20] As a result, the presence of the mid-gap states can be observed using scanning tunneling microscopy (STM) even following brief air exposure of the samples.[19] This improved chemical stability and electrical activity of the surface are essential for ex-situ processing using the self-assembly techniques.

As reported earlier, non-alloyed ohmic contacts are potentially useful for nano-device applications since they are free from a deep interface and they possess high spatial uniformity.[9] Since the conventional contacts such as alloyed Au/Ge/Ni on n-type GaAs are spatially nonuniform and also consume a significant surface layer in order to provide suitably low specific contact resistivity,[21] this requirement presents significant problems for nanocontacts based on any alloying process. Low resistance non-alloyed contacts to

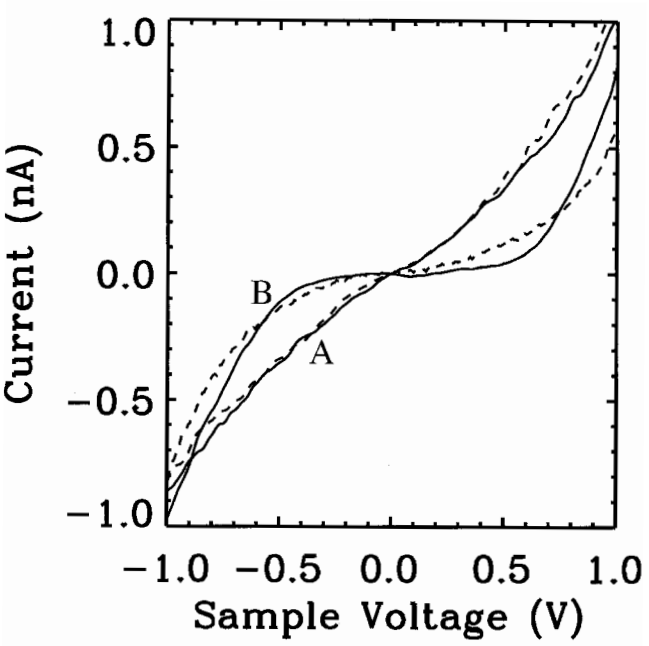

Fig. 2. I(V) data taken with the STM tip positioned over the Au cluster (curves A) and over the XYL-coated substrate (curves B) with a fixed tip position determined by V_{set} = –1.0 V and I_{set} = 0.8 nA. Data for samples with p-doped LTG:GaAs layer and undoped LTG:GaAs layer are indicated by solid and dashed curves, respectively.

n-GaAs can be realized by employing a surface layer of LTG:GaAs. Large area ex-situ, non-alloyed ohmic contacts employing a chemically stable LTG:GaAs surface layer can provide a specific contact resistance (ρ_c) below 1×10^{-6} $\Omega \cdot cm^2$.[22]

The GaAs layer structure used in this study, shown in Fig. 1, employs a thin (10 nm) layer of LTG:GaAs to facilitate a high quality nanocontact to n-GaAs(100) layers grown at standard temperatures. Two wafers were prepared with the same vertical structures except for the doping in the LTG:GaAs cap layer: one is undoped LTG:GaAs (n-type) and the other is p-doped LTG:GaAs (Be-doped at 2×10^{20} cm^{-3}).

The controlled-geometry nanocontacts are obtained by depositing isolated Au clusters with diameters of ~4 nm onto the LTG:GaAs based ohmic contact structures using ex-situ chemical self-assembly techniques. To form a reliable electrical contact at the nanoscale, a SAM of XYL is used to tether Au nanoclusters to the LTG:GaAs surface. The XYL SAM is grown by immersing the LTG:GaAs substrate in a ~1 mM solution of XYL in acetonitrile in a nitrogen atmosphere for 12–18 h, followed by thorough rinsing in acetonitrile. Finally, dodecanethiol encapsulated Au nanoclusters are deposited by casting a few drops of the Au colloidal solution on the substrate. The XYL molecules on the substrate displace part of the dodecanethiol molecules surrounding each Au cluster and chemically bond the cluster to the substrate. The resulting structure of the nanocontact is shown in Fig. 1.

X-ray photoemission spectroscopy (XPS) measurements of undoped LTG:GaAs (uncoated with XYL) indicate that the time constant for significant oxidation of the surface is longer than one hour at atmosphere.[20] During nanocontact fabrication, the surface oxide is stripped using HCl immediately before the sample is coated with XYL. Based on the behavior of large area contacts and the nanocontact structure, it appears that this oxide strip temporarily restores the surface Fermi level to an unpinned condition. The prompt deposition of the XYL monolayer in a dry nitrogen glovebox appears to provide passivation against significant re-oxidation. A separate ellipsometric study indicates that p-doped LTG:GaAs is more stable against oxidation than undoped LTG:GaAs when exposed to air and that the XYL-coated LTG:GaAs (either undoped or p-doped) is a stable surface.[9] It is believed that the sulfur to GaAs bond provides passivation comparable to that observed in studies involving elemental sulfur, with additional stability provided both by the characteristics of the LTG:GaAs and the organic tail of the XYL molecule.[23–25] A patterned XYL layer has been used as an etch mask for wet chemical etching of the GaAs layers by covering these molecules in certain areas of the sample surface.[26]

RESULTS AND DISCUSSION

A UHV STM was used to locate nanoclusters and probe the electronic properties of the nanocontacts. The UHV STM used in this study was obtained from Park Scientific Instruments. The STM tip is mounted on an orthogonal XYZ piezo-tripod having a calibration of 1.4 nm/V. The head is housed in an ion-pumped chamber with a pressure less than 2×10^{-9} torr as measured by a nude ion-gauge. The tips employed in this study were made by cutting Pt/Ir wires (diameter 0.2 mm) with a clean pair of wire cutters. Transmission electron microscope (TEM) micrographs of STM tips revealed that the end of the cut tip was sharp with a typical diameter of less than 20 nm.

Figure 2 shows representative I(V) data for cases where the STM tip was positioned (i) over a Au nanocluster (curves marked "A") and (ii) over the XYL-coated LTG:GaAs surface (curves marked "B"). Data are presented for two samples; one with a p-doped LTG:GaAs cap layer (solid curves) and the other with an undoped LTG:GaAs cap layer (dashed curves). I(V) measurements were performed at a fixed tip position over the sample determined by a set voltage V_{set} and a set current I_{set}. When I(V) was measured over a Au cluster, the data exhibited an ohmic behavior with a significant enhancement in the conduction for low bias voltages compared to I(V) data measured over the XYL-coated substrate, regardless of the dopant type of LTG:GaAs cap layer.

The ohmic behavior is found to persist to higher tunnel currents when the tip is positioned over a Au cluster, as shown in Fig. 3. The solid curves correspond to a nanocontact with a p-doped LTG:GaAs cap layer and the dashed curves correspond to a nanocontact with an undoped LTG:GaAs cap layer. Different set conditions determine a different tip position over the sample. A larger I_{set} represents a closer tip position to the sample. When a nanocontact structure with an undoped LTG:GaAs cap layer is probed,

ohmic I(V) characteristics were observed up to ~30 nA. When I(V) measurements were attempted at larger current levels, the STM tip was observed to dislodge the Au cluster. For these high currents, the STM tip comes so close to the cluster that it mechanically damages the nanocontact. For the case of a nanocontact with a p-doped cap layer, the ohmic behavior persists to higher tunnel currents (up to 200 nA) without damaging the Au cluster.

The specific contact resistance (ρ_c) of this ohmic contact can be estimated due to the well-characterized, single crystal Au nanoclusters used in this study. From geometrical considerations, the area A of a Au(111) facet on a ~4 nm high, truncated octahedral cluster is $\sim 9 \times 10^{-14}$ cm^2. In order to determine realistic limits on ρ_c and maximum current capability of the nanocontact, a technique measuring I versus the tip-cluster spacing, (I(z)) is utilized.[9] As the tip approaches the cluster, the tip-to-cluster resistance decreases and eventually becomes negligible, so the current will saturate at a value dictated by the applied voltage V, and the resistance between the cluster and the semiconductor substrate. The latter resistance is the contact resistance for the nanocontact. The corresponding ρ_c can then be found from (V/I)A in this regime. The I(z) data from the undoped LTG:GaAs cap layer was discussed in the previous study.[9] From this method, a ρ_c of $\sim 1 \times 10^{-6}$ Ω·cm^2 and a maximum current density, J_{max} of $\sim 1 \times 10^6$ A/cm^2 were determined for this nanocontact. For the nanocontact structure with a p-doped LTG:GaAs cap layer, the I(z) did not saturate.

The log(I) vs z relationship remained roughly linear up to 1000 nA, the measurement limit of our system.[27] Using this maximum current value, we determined an upper bound for ρ_c of $\sim 1 \times 10^{-7}$ Ω·cm^2 and a lower bound for J_{max} of $\sim 1 \times 10^7$ A/cm^2 for the nanocontact with the p-doped LTG:GaAs cap layer.[27] The difference in the contact properties between the samples can be qualitatively explained by the better surface stability of p-doped LTG:GaAs and the presence of mid-gap states near the Fermi level in this material.[26,27] The I(V) shape difference between measurements over the cluster and over the XYL-coated surface can also be qualitatively explained by the work function difference between the Au nanocluster and the Pt/Ir tip and the resulting surface barrier height difference between the two cases.

The performance of the nanocontact can be modeled by extending a quantitative model[28] for the large-area contact structure employing a LTG:GaAs surface layer.[22] In the large area contact, the conduction mechanism is primarily tunneling (field-emission and/or thermionic field emission) from the metal into the n++ layer. In the case of the nanocontact, the tunnel barrier for conduction between the metal and the n+ GaAs layer consists of the thin (1 nm) organic tether molecule, the LTG:GaAs cap layer and a portion of the n++ GaAs layer. While the limiting conduction mechanism is still thought to be tunneling, it is possible that conduction through the mid-gap band of defect states also plays a role in the structure with the

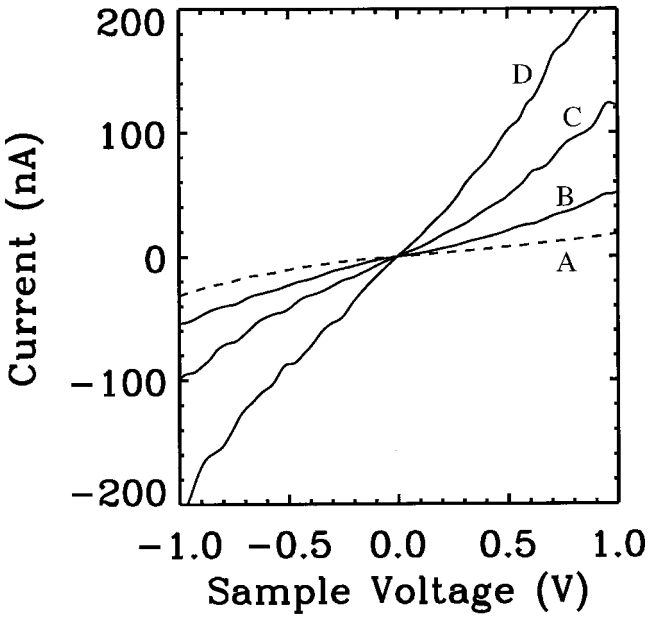

Fig. 3. I(V) data taken over Au cluster on a sample with undoped LTG:GaAs with V_{set} = -1.0 V and I_{set} = 30 nA (A, dashed) and a sample with p-doped LTG:GaAs (solid curves) with V_{set} = –1.0 and I_{set} = 50 nA (B), 100 nA (C), and 200 nA (D). Different set conditions determine a different tip position over the sample. A larger I_{set} represents a closer tip position to the sample.

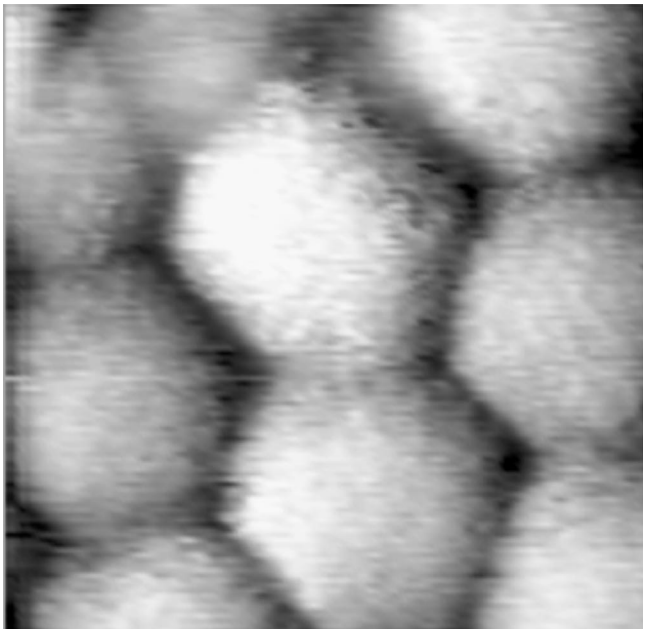

Fig. 4. A 17 × 17 nm UHV STM topographic image of close-packed 2-D array of Au nanoclusters tethered to the XYL-coated p-doped LTG:GaAs, acquired with V_{set} = –1.5 V and I_{set} = 0.15 nA. The high resolution image indicates faceted geometry of cluster.

p-doped LTG:GaAs cap. The low specific contact resistance indicates that the energy barrier at the GaAs surface is well below the 0.7 eV barrier which would be expected if mid-gap surface Fermi level pinning occurs. Since the mid-gap surface pinning is associated with surface states arising from oxidation, the unpinned surface Fermi level indicates that there is a relatively low surface state density at the GaAs

surface and therefore that the surface is not significantly oxidized. This finding reflects the chemical stability provided by the combination of a chemically stable semiconductor surface layer (LTG:GaAs) and the additional passivation effects of the XYL SAM. Although the nanocontact is assembled via ex-situ processing, good control of the surface electrical properties and coupling has been achieved.

The self-assembled nanocontact structure represents a self-aligned metallic node/device interface. We have seen evidence that a metallic nanocluster can be used as an etch mask for defining a semiconductor mesa. In this case, the nanocluster becomes a self-aligned ohmic contact structure to the device mesa. If the mesa incorporates a heterostructure device layer, the ohmic nanocontact structure can provide a unit cell structure for a nanoelectronic circuit configuration. The UHV STM image of Fig. 4 shows a portion of a hexagonal close-packed 2-D array of Au nanoclusters tethered to the XYL-coated p-doped LTG:GaAs. The detail fabrication procedure is presented elsewhere.[10] This high resolution image indicates the faceted geometry of the clusters and the excellent local ordering provided by the self assembly technique. Similar characterization on an array sample deposited on a ohmic contact structure containing a p-doped LTG:GaAs layer indicates that the strong coupling into the semiconductor substrate through the molecular tether (XYL) is also observed for the clusters within the array. The configuration of a locally-connected 2-D network of metallic nodes coupled to an active substrate (e.g., resonant tunneling diode structure) can provide the basis for a computational cell of a nanoelectronic circuit.[29] It is expected that the current work can be extended to realize arrays of device mesas defined by linked metallic nanoclusters.

CONCLUSION

In conclusion, we have described an approach in which we combine self-assembled metal/molecule nanostructures with chemically stable semiconductor surface layers. As a result, high quality interfaces and controlled nanometer scale structures can be realized. With this hybrid technique, we have developed and characterized a nanometer scale, ohmic contact to n-GaAs using a Au cluster/XYL/GaAs structure. Au nanoclusters are found to be well tethered to the LTG:GaAs substrate by a monolayer of XYL molecules. The I(V) characteristics of the Au cluster/XYL/GaAs nanocontact exhibit an ohmic behavior with specific contact resistance of $\sim 1 \times 10^{-7}\ \Omega\cdot cm^2$ and maximum current density of $\sim 1 \times 10^7$ A/cm^2, both comparable to those observed from large area contacts. In addition, a 2-D array of Au nanoclusters has been fabricated on the GaAs surface and characterized using STM. These structures are of potential interest for nanoelectronic device applications.

ACKNOWLEDGEMENTS

This work was partially supported by DARPA/Army Research Office under Grant DAAH04-96-1-0437, NSF MRSEC program under Grant 9400415-G-0144, and AFOSR grant F49620-96-1-0234A. We would like to thank S. Datta, C.P. Kubiak, B. Kasibhatla, J. Lauterbach, and S. Howell for many helpful discussions throughout the course of this work.

REFERENCES

1. D.J. Eaglesham and M. Cerullo, *Phys. Rev. Lett.* 64, 1943 (1990).
2. P.C. Sharma, K.W. Alt, D.Y. Yeh, D. Wang, and K.L. Wang, *J. Electron. Mater.* 28, 432 (1999)
3. S. Bandyopadhyay, L. Menon, N. Kouklin, H. Zbeng, and D.J. Sellmyer, *J. Electron. Mater.* 28, 515 (1999).
4. R.P. Andres, J.D. Bielefeld, J.I. Henderson, D.B. Janes, V.R. Kolagunta, C.P. Kubiak, W.J. Mahoney, and R.G. Osifchin, *Science* 273, 1690 (1996).
5. C.B. Murray, C.R. Kagan, and M.G. Bawendi, *Science* 270, 1335 (1995).
6. S. Facsko, T. Dekorsy, C. Koerdt, C. Trappe, H. Kurz, A. Vogt, and H.L. Hartnagel, *Science* 285, 1551 (1999).
7. L.C. Brousseau, III, J.P. Novak, S.M. Marinakos, and D.L. Feldheim, *Adv. Mater.* 11, 447 (1999).
8. R.P. Andres, T. Bein, M. Dorogi, S. Feng, J.I. Henderson, C.P. Kubiak, W. Mahoney, R.G. Osifchin, and R. Reifenberger, *Science* 272, 1323 (1996).
9. T. Lee, J. Liu, D .B . Janes, V.R. Kolagunta, J. Dicke, R. P. Andres, J. Lauterbach, M.R. Melloch, D. McInturff, J.M. Woodall, and R. Reifenberger, *Appl. Phys. Lett.* 74, 2869 (1999)
10. J Liu, T. Lee, B.L. Walsh, R.P. Andres, D.B. Janes, M.R. Melloch, J.M. Woodall, and R. Reifenberger, in progress.
11. R.S. Bowles, J.J. Kolstad, J.M. Calo, and R.P. Andres, *Surf. Sci.* 106, 117 (1981).
12. M. Brust, M. Walker, D. Bethell, D.J. Schiffrin and R. Whyman, *J. Chem. Soc. Chem. Commun.* 1994, 801 (1994).
13. D.A. Handley, *Colloidal Gold: Principles, Methods, and Applications,* vol. 1, ed. M.A. Hayat (San Diego, CA: Academic Press, 1989), Chap. 2.
14. B.O. Dabboussi, C.B. Murray, M.F. Rubner, and M.G. Bawendi, *Chem. Mater.* 6, 216 (1994).
15. J.R. Heath, C.M. Knobler, and D. V. Leff, *J. Phys. Chem. B* 101, 189 (1997).
16. A. Ulman, editor, *Thin Films: Self-Assembled Monolayers of Thiols,* vol. 24 (San Diego, CA: Academic Press, 1998).
17. M.J. Lercel, M. Rooks, R.C. Tiberio, H.G. Craighead, C.W. Sheen, A.N. Parikh, and D.L. Allara, *J. Vac. Sci. Technol. B* 13, 1139 (1995); M.J. Lercel, H.G. Craighead, and D.L. Allara, *Appl. Phys. Lett.* 68, 1504 (1996).
18. M.R. Melloch, J.M. Woodall, E.S. Harmon, N. Otsuka, F.H. Pollak, D.D. Nolte, R.M. Feenstra, and M.A. Lutz, *Annl. Rev. Mater. Sci.* 25, 547 (1995).
19. S. Hong, D.B. Janes, D. McInturff, R. Reifenberger, and J.M. Woodall, *Appl. Phys. Lett.* 68, 2258 (1996).
20. T.-B. Ng, D.B. Janes, D. McInturff, and J.M. Woodall, *Appl. Phys. Lett.* 69, 3551 (1996).
21. A.G. Baca, F. Ren, J.C. Zopler, R.D. Briggs, and S.J. Pearton, *Thin Solid Films* 308-309, 599 (1997).
22. M.P. Patkar, T.P. Chin, J.M. Woodall, M.S. Lundstrom, and M.R. Melloch, *Appl. Phys. Lett.* 66, 1412 (1995).
23. O.S. Nakagawa, S. Ashok, C.W. Sheen, J. Martensson, and D.L. Allara, *Jpn. J. Appl. Phys.* (Part. 1) 30, 3759 (1991).
24. S.R. Lunt, G.N. Ryba, P.G. Santangelo, and N.S. Lewis, *J. Appl. Phys.* 70, 7449 (1991).
25. J.F. Dorsten, J.E. Maslar, and P.W. Bohn, *Appl. Phys. Lett.* 66, 1755 (1995).
26. D.B. Janes et al., *J. Vac. Sci. Technol.* B 17, 1773 (1999).
27. T. Lee, N.-P. Chen, J. Liu, R.P. Andres, D.B. Janes, E.H. Chen, M.R. Melloch, J.M. Woodall, and R. Reifenberger, *Appl. Phys. Lett.* 76, 212 (2000).
28. N.-P. Chen, H.J. Ueng, D.B. Janes, J.M. Woodall, and M.R. Melloch, *J. Appl. Phys.* (in press).
29. V.P. Roychowdhury, D.B. Janes, S. Bandyopadhyay, and X. Wang, *IEEE Trans. Electron. Dev.* 43, 1688 (1996).